Surface States of Charge Carriers and Electrical Properties of the Surface Layer of Ice

Victor F. Petrenko* and Ivan A. Ryzhkin†

Thayer School of Engineering, Dartmouth College, Hanover, New Hampshire 03755

Received: October 11, 1996[⊗]

We propose a theoretical model that successfully describes numerically such major features of the electrical conductivity of the surface of ice as its magnitude and frequency dependence. Comparison of the model with experimental results on σ_s confirms that the magnitudes of the ice surface charge density and ice surface potential are close to those observed in independent measurements. The model predicts the thickness of an electric double layer which is comparable with the experimentally observed thickness of the liquidlike layer on ice (∼5 nm at −10 °C). This coincidence raises a question about the role of electrostatic pressure and possible superionic transition in the specific structure and properties of the surface of ice.

1. Introduction

In this paper we develop a theoretical model that describes ice surface conductivity, surface charge density, and surface potential. The electrical properties of ice play decisive or otherwise important roles in such natural phenomena as thunderstorm electricity, ice frictional electrification,[1] and ice friction and adhesion,[2] and of course, they account for the very high surface conductivity of ice.[3] For these reasons the electrical properties of ice have been under intensive experimental investigation for the past several decades. Readers can find a comprehensive review of the results in the recent monograph by Petrenko.[4]

In numerous experiments, researchers have studied surface conductivity, surface charge density, surface potential, and mobilities of charge carriers in the ice surface. Much less attention has been paid to the theoretical interpretation of these data. Although there are several theoretical models whose aim is to describe the structure and thermodynamics of the surface of ice (see, for example, refs 5−8), none of the authors of these models have tried to describe the electrical properties of ice surface. The existing theoretical models of ice surfaces have also failed to describe the combination of unusual properties of the ice surface: its high electric conductivity, high self-diffusion coefficient, and the existence of a liquidlike layer on the ice surface at temperatures as low as −100 °C,[9] among other properties.

We will show that most of the important electrical properties of the surface of ice can be explained within the framework of our current understanding of charge transport in ice, when the latter is combined with the phenomena of surface states developed in the study of the physics of semiconductors. We will calculate the space charge density in the subsurface layer of ice, surface potential with respect to the ice bulk, and surface conductivity. Then we will compare our theoretical results with available experimental data and discuss the effect of the surface charge on the premelting and subsurface structure.

2. Model and Basic Equations

In the Jaccard theory, the electrical charge is transferred by protonic point defects: H_3O^+, OH^-, D, and L, which play a role similar to electrons and holes in electronic semiconductors. Their creation energies are $E_{12} = 1$ eV and $E_{34} = 0.68$ eV for (H_3O^+, OH^-) and (D, L) pairs, respectively, and those energies do not depend on position within a uniform and infinitely large crystal. Where an ice crystal has a surface, some of the protonic defects may be captured in the surface states which have energies lower than those in the bulk of the ice. The capture of charged protonic defects in the surface states will result in buildup of the surface charge, surface electric field, and configuration vector. Surface electric charge can also be generated either by absorption of ions from air, due to an imbalance in the nubmer of positive and negative ions dissolved in the ice, or by an applied external electric field. Whatever the reason for the surface charge, it will be screened by intrinsic charge carriers. The screening region of increased concentration of defects will have high electric conductivity and a much more movable protonic system. The latter is presumed to lead to very high self-diffusion coefficients, plasticity, and other unusual properties.[10,11]

The centerpiece of our model is the assumption of a high-density surface charge sitting on ice/vapor and ice/solid interfaces. There is convincing experimental and theoretical evidence for such a surface charge on ice. In the case of an ice/vapor interface, the surface charge results from partial ordering of water molecules on the ice surface. Such ordering had first been suggested for ice by Fletcher,[5] who calculated interactions between dipole and quadrupole moments of water molecules close to the surface. This ordering of water molecules induces an electrical polarization which has a maximum on the surface but gradually decays with distance into the ice bulk. Such spatial distribution of polarization $\vec{P}$ is equivalent to specific distribution of a subsurface space charge ρ, due to well-known relation between them:

$$\rho = -\nabla \cdot \vec{P} \tag{1}$$

For instance, if, as Fletcher deduced, water molecules on the surface are oriented with their protons outward, then there is a high-density positive surface charge and a negative subsurface space charge screening the former one. Computer simulation of the molecular structure in the ice subsurface layer, though it differs from Fletcher's theory in numbers, confirmed the partial ordering of water molecules on the ice surface.[12]

On ice/metal and ice/dielectric interfaces, there is one more reason for the surface charge to build up. This is an electrostatic attraction, known as an image force, of mobile ions and Bjerrum defects to the interface, if the solid in contact with ice has an

* To whom correspondence should be addressed.

† On leave from the Institute of Solid State Physics of the Russian Academy of Sciences.

⊗ Abstract published in *Advance ACS Abstracts,* June 15, 1997.

S1089-5647(96)03216-6 CCC: $14.00

effective dielectric constant ϵ larger than that for ice ϵ_∞. Such an image force F is inversely proportional to the square of the distance to the interface z:

$$F = \frac{q^2}{16\pi\epsilon_0\epsilon z^2}\frac{\epsilon_\infty - \epsilon}{\epsilon_\infty + \epsilon} \tag{2}$$

At large distances from the interface, the image forces are the same for positive and negative protonic charge carriers in ice. At small distances that are comparable with molecular size, however, the forces may differ for positive and negative defects, due to the fact that the wave function of a positive defect (proton) is much more compact than that for a negative defect (which includes electrons). This difference will result in differing depth of surface states for positive and negative defects as well as differing occupancy, thus generating a net surface charge. Calculation of the occupancy coefficient of the surface states in ice is given in our second paper (13) published in this proceedings. Finally, the third reason for a surface charge on ice contacting a solid is the difference in work functions of the two materials, i.e., a contact potential.

Evidence of the ice surface charge has been found in experiments on ice surface potential[14−16] and from observations of ice frictional electrification.[1] Whatever the reason for such a surface charge, we will consider it as a parameter in this paper. The surface charge induces a layer of unlike space charge of mobile protonic charge carriers. This screening of charge carriers is responsible for the high surface conductivity of ice.

A detailed description of the electric structure near the ice surface includes calculations of the electrostatic potential $\varphi(z)$, potential function $\chi(z)$ of a configurational vector $\mathbf{\Omega}(z)$, $\mathbf{\Omega} = -\mathrm{d}\chi/\mathrm{d}z$, and concentrations of the defects per one water molecule $n_\alpha(z)$, where $\alpha = 1$, 2, 3, and 4 labels H_3O^+, OH^-, D, and L defects, respectively. The equations for φ and χ can be written in the following form:

$$\frac{\mathrm{d}^2\varphi}{\mathrm{d}z^2} = -\frac{N}{\epsilon\epsilon_0}\sum_{\alpha=1}^{4} e_\alpha n_\alpha \tag{3}$$

$$\frac{\mathrm{d}^2\chi}{\mathrm{d}z^2} = N\sum_{\alpha=1}^{4}\eta_\alpha n_\alpha \tag{4}$$

where N is a concentration of water molecules, ϵ and ϵ_0 are the high-frequency dielectric permittivity of ice and the dielectric permittivity of a vacuum respectively, e_α is the effective charge of the various defects ($0.62e$, $-0.62e$, $0.38e$, $-0.38e$), and $\eta_\alpha = (1, -1, -1, 1)$. The first equation is the Poisson's equation and the second one can be obtained from the definition of a configuration vector.[17] At infinity on the ice side, both φ and χ vanish, but at the surface their first derivatives are given by the surface densities of defects:

$$\frac{\mathrm{d}\varphi(0)}{\mathrm{d}z} = -\frac{\sqrt{3}}{4r_{OO}^2\epsilon\epsilon_0}[e_1(f_1 - f_2) + e_3(f_3 - f_4)] \tag{3a}$$

$$\frac{\mathrm{d}\chi(0)}{\mathrm{d}z} = \frac{\sqrt{3}}{4r_{OO}^2}(f_1 - f_2 - f_3 + f_4) \tag{4a}$$

where f_α is the number of defects at the surface state per water molecule and r_{OO} is the distance between two adjacent oxygen atoms.

To make the system of eq 3 and 4 closed, we have to add equations expressing n_α in term of electrostatic potential and configuration vector. This is not trivial, because we have to use a general expression which must be valid even for concentrations of defects comparable with the concentration of water molecules. Let us consider first the case of $\varphi = 0$ and $\chi = 0$. Taking into account calculations of the entropy of ice with ionic and Bjerrum defects,[18] we can express the free energy of ice in the following form:

$$F = F_{1,2} + F_{3,4} \tag{5}$$

$$F_{1,2} = (E_{12}/2)n_{1,2} + kT[n_{1,2}\ln n_{1,2} + (^1/_2 - n_{1,2})\ln 2(1 - 2n_{1,2})/3] \tag{6}$$

$$F_{3,4} = (E_{34}/2)n_{3,4} + kT[n_{3,4}\ln n_{3,4} + (1 - n_{3,4})\ln(1 - n_{3,4})] \tag{7}$$

Minimizing the free energy with respect to n_α, we arrive at the following equations:

$$n_{1,2} = \frac{^2/_3}{\exp(E_{12}/2kT) + {}^4/_3} \qquad n_{3,4} = \frac{1}{\exp(E_{34}/2kT) + 1} \tag{8}$$

It is interesting to note here that the fact that Bjerrum defects obey the Fermi statistics is really the consequence of an obvious restriction: there can be only one Bjerrum defect on each hydrogen bond. However, the ionic defects are described by deformed (or fractional) statistics which are closer to the Fermi one. For the nonzero electric and configuration fields, we have to modify the arguments of the exponential functions in eq 8:

$$E_{12}/2kT \rightarrow E_{12}/2kT + \psi_{1,2} \qquad E_{34}/2kT \rightarrow E_{34}/2kT + \psi_{3,4} \tag{9}$$

where $\psi_a = (e_\alpha\varphi - \eta_\alpha\Phi\chi)/kT$, $\Phi = 8r_{OO}kT/3^{1/2}$, and r_{OO} is the distance between the closest oxygen atoms.

Equations 3, 4, 8, and 9 form a closed system, but it can be simplified significantly if we neglect the configuration vector. Let us estimate the contribution of the configuration vector into ψ_α. Using definition of ψ_α and eqs 3 and 4, we obtain a parameter ξ:

$$\xi = \Phi\chi/e_3\phi \approx \Phi\epsilon\epsilon_0/e_3^2 \approx \frac{8kT}{\sqrt{3}(e_3^2/\epsilon\epsilon_0 r_{OO})} \approx 0.035 \tag{10}$$

where we used the least effective charge to get the largest possible value of the parameter ξ. (For ionic defects it is even less.) Since this parameter is small, in zero approximation with respect to ξ, we will neglect the effect of the configuration vector and use the shortened system of eqs 3, 8, and 9 and set $\chi = 0$ into the definition of ψ_α. The system of equations then can be immediately integrated once, and we finally come to the first-order differential equation:

$$\mathrm{d}\psi/\mathrm{d}t = -\sqrt{f_1(\psi)\, f_1(-\psi) f_2^2(\psi)\, f_2^2(-\psi)} \tag{11}$$

where $\psi = e_3\varphi/kT$, $t = z/\lambda$, $\lambda = (\epsilon\epsilon_0 kT/(e_3)^2N)^{1/2}$, and the functions f_1 and f_2 are defined by the equations

$$f_1(\psi) = \frac{\exp(E_{12}/2kT) + (4/3)\exp(\gamma\psi)}{\exp(E_{12}/2kT) + 4/3}$$

$$f_2(\psi) = \frac{\exp(E_{34}/2kT) + \exp(\psi)}{\exp(E_{34}/2kT) + 1} \tag{12}$$

with $\gamma = e_1/e_3$ and $\mathrm{d}\psi(0)/\mathrm{d}t = (e_3\lambda/kT)(\mathrm{d}\varphi(0)/\mathrm{d}z)$. By solving

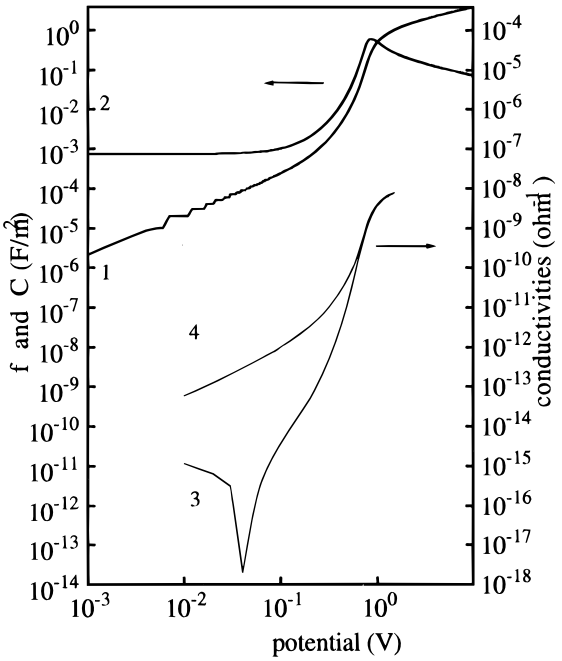

Figure 1. Graph showing the dependence of the occupancy coefficient f (number of captured D defects per one surface molecule; curve 1) and differential capacity of subsurface layer per unit surface $C(V) = dQ/dV$ (curve 2) vs the surface potential V for the case in which D defects are captured in the surface states. The values $f > 1$ correspond to the applied external voltage (external charges). Curves 3 and 4 depict the low- and high-frequency surface conductivities. (The zero points of the conductivities have been chosen at the minimum of low-frequency conductivity, temperature −10 °C.)

eq 11, we can find the electrostatic potential ψ, which is used in calculations of local concentrations and therefore local conductivities, using eqs 8 and 9. Moreover, by inserting the local concentrations into eq 4, we can find χ and check whether the effect of the configuration vector is really negligible.

3. Numerical Procedure and Results

For certainty, we assume now that the physical reason for the electric field near the ice surface is occupancy of the surface states by D defects, which means $f_1 = f_2 = f_4 = 0$ and $f_3 \neq 0$. The occupancy coefficient, f_3, defines the surface charge density and surface electric field and therefore the first derivative of ψ at the surface. Equation 8, taken at $t = 0$, can be considered an algebraic equation with respect to the surface potential φ_s. Its solution provides us with the surface potential as a function of the occupancy coefficient, f_3, and is pictured in Figure 1 as curve 1. Curve 2 depicts the electrical capacity of the electric double layer, $C(\varphi_s) = dQ/d\varphi_s$. Note the large value of the capacity for φ_s in the interval from 0.1 to 1.0 V, indicating a dramatic increase in the surface charge within this interval of surface potential. The upper limit value of $f_3 = 1$ corresponds to the surface potential of about 1.5 V. However, because of Coulomb interaction between the D defects on the surface, the more probable value of occupancy is about 0.1, with a corresponding surface potential $\varphi_s = 0.75$ V.

All remaining calculations are reduced to a calculation of space dependence of the electrostatic potential $\varphi(z)$ under different conditions, calculations of local conductivities of thin subsurface layers, and then summation over these layers. Doing so, we obtain the voltage dependence of the low- and high-frequency surface conductivities (Figure 3, curves 1 and 4), and also the temperature dependence of these conductivities when the occupancy coefficient remains constant at $f_3 = 0.1$. We used the following values for the mobilities: $\mu_1 = 9 \times 10^{-8}$, $\mu_2 = 2.7 \times 10^{-8}$, $\mu_3 = 10^{-9}$, and $\mu_4 = 1.8 \times 10^{-8}$ (in $m^2/V \cdot s$).[19,20]

First, we have to emphasize that our theoretical results for the low-frequency surface conductivity of ice fall inside the range of experimentally observed surface conductivities. Measured values of low-frequency surface conductivity have been found to be in the range between 10^{-11} and 10^{-9} Ω^{-1}.[3,21,22] Such a magnitude of σ_s would correspond to the occupancy coefficient in the interval 0.01−0.14 and would correspond to the ice surface potential from 0.52 to 0.78 V. As noted previously, these are the most probable values of the occupancy coefficient and the surface potential. Furthermore, we can now use our results to predict how the surface conductivity depends on a dc bias applied from outside. For instance, if we applied a positive potential to ice, we would get an increase in both the surface charge and the surface conductivity. For a negative potential, we would get lowering of the surface conductivity down to its bulk magnitude when the applied voltage compensated for the built-in surface potential. Then the conductivity would begin to increase again. We should note also that at a very high dc bias applied to the ice surface it is possible to reach some sort of saturation point. As one can see in Figure 1, the capacity of the subsurface layer begins to decrease above 1 V. This means that, in spite of the voltage increase, the growth velocity of the surface charge slows down. It is also interesting to note that at very low voltage the surface conductivity decreases as the voltage increases. This happens because defects of highest mobility (H_3O^+) are expelled from the screening layer, and this process dominates the increase in concentration of negative defects (OH^- and L). Then, however, the increase in a number of negative defects becomes too large and begins to play the major role.

We found a slow temperature dependence of the surface conductivities under the condition of a fixed value of the surface charge. This is quite natural. In fact, the fixed value of the surface charge keeps the screening charge constant. If all defects had equal mobilities, then the conductivity should be constant. We should emphasize, however, that this conclusion is a direct consequence of using temperature-independent mobilities, which is not the real case.

We plan to investigate temperature dependence in the future; here, we just note reasons which could give a strong temperature dependence of the surface conductivity. First is the temperature dependency of defect mobilities (which are currently known only for H_3O^+ and L defects). Second is the temperature dependence of the occupancy coefficient, and third is the possibility of localization of charge carriers in the lateral direction under the action of a nonuniform surface potential. We also found that in the most interesting range of f_3 the difference between the high- and low-frequency surface conductivities is smaller than that for ice bulk conductivities. This is illustratedin Figure 2, which also depicts the frequency dependence of real and imaginary parts of the surface conductivity.

Finally, what is the width of a layer that provides the main contribution to the surface conductivity? In answering this question, one has to be very careful and distinguish different quantities. For example, the electrostatic potential decays rather slowly (it is about 10^{-3} φ_s at $z = 800r_{OO}$), while the defect concentrations decrease very rapidly, so that a subsurface layer of $6r_{OO}$ thickness gives 95% of the whole conductivity. Moreover, the width of this relevant layer decreases as the surface potential increases.

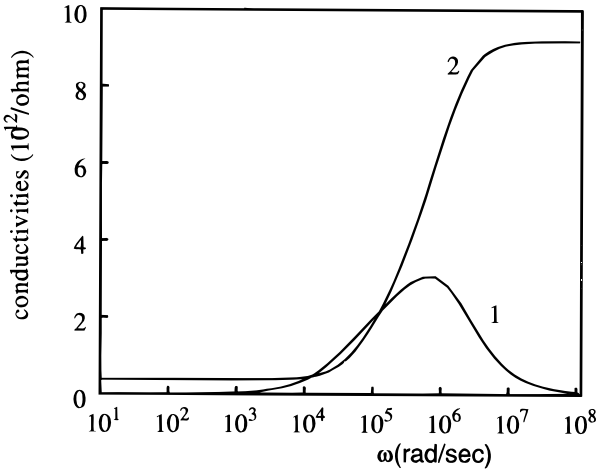

Figure 2. Curves 1 and 2 depict the imaginary and real parts of the conductivity vs angular frequency ω: $T = -10$ °C, $f_3 = 0.0016$ ($V_s = 0.3$ V).

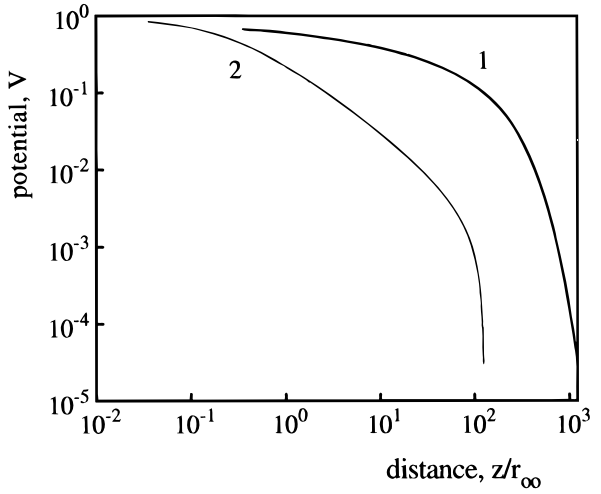

Figure 3. Graph showing the space dependence of the electrostatic potential (curve 1) and the fraction of screening defects outside the layer of thickness z (curve 2).

4. Other Mechanisms and Approximations

The basic approximation used in our calculations neglected the role of the configuration vector. The simplified estimate showed that the expected error did not exceed the parameter $\xi \approx 0.035$. More strictly, we should insert the found space-dependent concentrations into eq 4, integrate the latter, and then recalculate all the quantities using eqs 8 and 9. We performed this procedure and proved that all the corrections are of the order of ξ. One more restriction that must be checked is the values of concentrations just near the surface. In fact, at large values of surface potential (above ~0.8 V), the near-surface concentration of defects becomes so high that the local length of screening is comparable with intermolecular distances. Under this condition our continuous theory fails, and it is necessary to take into account the discreteness of the charge distribution. Almost all screening in this case is performed within a very thin layer (several molecular slices), and actually we come to the double electric layer.

If for some reason the subsurface layer of ice undergoes a phase transition, the model described above should be modified. For instance, even at concentrations much lower than the molecular one, there could occur a superionic transition with a sharp increase in concentration of defects.[18] It brings a screening layer of approximate width f_3/n_{si}, where n_{si} is the defect concentration within the superionic layer. The superionic layer would also have a sharp phase boundary with the bulk crystal. In the future we plan to study the effect of such a transition on the surface of ice. The prime question is whether the layer of very high concentration of defects is solid or liquid. There is strong experimental evidence of a liquidlike layer on ice/vapor and ice/solid interfaces. Such a layer was found in NMR experiments by Kvlividze et al.[23] and Mizuno and Hanafuza,[24] using optical ellipsometry by Furukawa et al.,[25,26] in glancing-angle X-ray scattering by Kouchi et al.[27] and Dosch et al.[28] and using scanning force microscopy by Nickolayev and Petrenko[29] and by Petrenko.[30] In the presence of such a liquidlike layer a part of the screening charge is localized inside the liquid (or quasi-liquid) layer. While in this case the whole ideology of calculations remains the same, numerical results may differ due to the different dielectric constants and activation energies of point defects in water and ice.

Finally, let us check whether electrostatic pressure generated by the electric double layer is capable of initiating pressure melting of the subsurface layer of ice. A simple estimate of electrostatic pressure in the top layer gives a value of about $p = f_3^2 e_3^2/S^2\epsilon\epsilon_0 \approx 4 \times 10^7$ Pa for $f_3 = 0.1$ (S being the surface per water molecule). According to the phase diagram of water, this pressure could decrease the melting point by -4 °C, but this pressure rapidly decays in the ice bulk: it drops by 1 order of magnitude at $z = 3r_{OO}$. For this reason the pressure melting could play an important role within a very thin layer and at temperatures close to the melting point. As we showed in our ice-adhesion paper (see this issue), under certain conditions the studied electric double layer can play a crucial role in the adhesion of ice to other solids.

5. Conclusions

1. We propose a model that successfully describes numerically such major features of the electrical conductivity of the surface of ice as its magnitude and frequency dependence. The model can qualitatively explain the strong dependence of surface conductivity on temperature.

2. Comparison of the model with experimental results on σ_s confirms that the magnitudes of the ice surface charge density and ice surface potential are close to those observed in independent measurements.

3. The model predicts the thickness of an electric double layer which is comparable with the experimentally observed thickness of the liquidlike layer on ice (~$20r_{OO}$ at -10 °C). This coincidence raises a question about the role of electrostatic pressure and possible superionic transition in the specific structure and properties of the surface of ice.

Acknowledgment. This research is supported by ARO under Grant DAAH04-95-1-0189. It was also supported in part by NSF under Grant DMR-9413362 and by ONR under Grant N00014-95-1-0621.

References and Notes

(1) Petrenko, V. F.; Colbeck, S. C. *J. Appl. Phys.* **1995**, *77*, 4518.
(2) Petrenko, V. F. *J. Appl. Phys.* **1994**, *76*, 1216.
(3) Maeno, N.; Nishimura, H. *J. Glaciol.* **1978**, *21*, 193.
(4) Petrenko, V. F. *The Surface of Ice*; US Army CRREL Special Report 94−22, 1994.
(5) Fletcher, N. H. *Philos. Mag.* **1968**, *18*, 1287.
(6) Fukuta, N. *J. Phys. C1* **1987**, *48*, 503.
(7) Dash, J. G. *Phase Transitions in Surface Films*; Taub, H., et al., Eds.; Plenum: New York, 1991; p 339.
(8) Elbaum, M.; Schick, M. *Phys. Rev. Lett.* **1991**, *66*, 1713.
(9) Mizuno, Y.; Hanafuza, N. *J. Phys. C1* **1987**, *48*, 511.
(10) Onsager, L.; Runnels, L. K. *J. Chem. Phys.* **1969**, *50*, 1089.
(11) Glen, J. W. *Phys. Kondens. Mater.* **1968**, *7* (1), 43.
(12) Kroes, G. J. *Surf. Sci.* **1992**, *275*, 365.

(13) Ryzhkin, I. A.; Petrenko, V. F. *J. Phys. Chem. B* **1997**, *101*, 6267.
(14) Mazzeta, E.; del Pennino, U.; Loria, A.; Mantovani, S. *J. Chem. Phys.* **1976**, *64*, 1028.
(15) Takahashi, T. *J. Atmos. Sci.* **1970**, *27*, 453.
(16) Petrenko, V. F. *Proceedings of the 11th International Symposium on Ice*; University of Alberta: Banff, 1992; p 1140.
(17) Petrenko, V. F.; Ryzhkin, I. A. *Phys. Status Solid: B* **1984**, *121*, 421.
(18) Ryzhkin, I. A. *Solid State Commun.* **1985**, *56*, 57.
(19) Petrenko, V. F.; Maeno, N. *J. Phys. C1* **1987**, *48*, 115.
(20) Jaccard, C. *Helv. Phys. Acta* **1959**, *32*, 89.
(21) Maeno, N. *Physics and Chemistry of Ice*; Whalley, E., Jones, S. J., Gold, L. W., Eds.; Royal Society of Canada: Ottawa, 1973; p 140.
(22) Maidique, M. A.; von Hippel, A.; Westphal, W. B. *J. Chem. Phys.* **1971**, *54*, 150.
(23) Kvlividze, V. I.; Kiselev, V. F.; Kurzaev, A. B.; Ushakova, L. A. *Surf. Sci.* **1974**, *44*, 60.
(24) Mizuno, Y.; Hanafuza, N. *J. Phys. C1* **1987**, *48*, 51.
(25) Furukawa, Y.; Yamamoto, M.; Kuroda, T. *J. Phys. C1* **1987**, *48*, 495.
(26) Furukawa, Y.; Yamamoto, M.; Kuroda, T. *J. Cryst. Growth* **1987**, *82*, 665.
(27) Kouchi, A.; Furukawa, Y.; Kuroda, T. *J. Phys. C1* **1987**, *48*, 675.
(28) Dosch, H.; Lied, A.; Bilgram, J. H. *Surf. Sci.* **1995**, *327*, 145.
(29) Nickolayev, O.; Petrenko, V. *Mater. Res. Soc. Proc.* **1995**, *355*, 221.
(30) Petrenko, V. F. *J. Phys. Chem. B* **1997**, *101*, 6276.